

MASSACHUSETTS INSTITUTE OF TECHNOLOGY  
DEPARTMENT OF MECHANICAL ENGINEERING  
CAMBRIDGE, MASSACHUSETTS 02139

2.002 Mechanics and Materials II  
Spring, 2004

Laboratory Module 3  
Sheet metal forming: elastic-plastic beam bending

## 1 Background and Objectives

In sheet metal forming operations, a sheet of metal is shaped into a product by plastic deformation. Typically, the sheet is deformed by forcing it to conform to the shape of a rigid die. Manufacturing processes commonly include:

- **Matched Die Forming**, in which the sheet is introduced between two matching male and female dies, and is deformed into the desired shape by bringing the two dies together.
- **Stretch Forming**, in which a sheet is clamped by the grips of a machine, stretched, and wrapped around a die.

The products manufactured by sheet-forming processes include a variety of shapes and sizes, ranging from simple bends to double-curvature parts, with shallow and deep recesses. Many of the major components of automobiles, aircraft, and large appliances are manufactured via sheet forming processes, as are the ubiquitous metal beverage/food containers.

Because of the elastic-plastic behavior of the sheet material, the deformation imposed on the sheet when it is forced to conform to the die has both *elastic* and *plastic* portions. The *plastic part* of the deformation is permanent, and it is not recovered when the sheet is unloaded by removing it from the die. The *elastic part* of the deformation is recovered upon removal of the load. This phenomenon is known as “**springback**”. In order to attain a desired part-shape, the shape of the die has to be designed so that it compensates for springback effects.

For complicated die shapes (*e.g.*, automotive quarter-panels), it is necessary to use numerical methods such as the finite element method in order to predict the shape that the part will assume when it is unloaded from the die. However, the basic concepts involved in die design and springback compensation are not difficult, and can be easily engaged at the 2.002 level, provided that the sheet and the die shapes are sufficiently simple. In this lab module, we will review elastic-plastic beam-bending theory and derive a procedure to predict springback for a metal strip loaded on a die with a single, constant curvature. Figure 1 schematically illustrates a matched die pair for imposing a single constant curvature. Figure 2 schematically illustrates the forming process, including (a) inserting the strip into the die, (b) closing the die onto the strip, and (c) the shape of the unloaded strip after the die has been opened and the strip removed from the die.

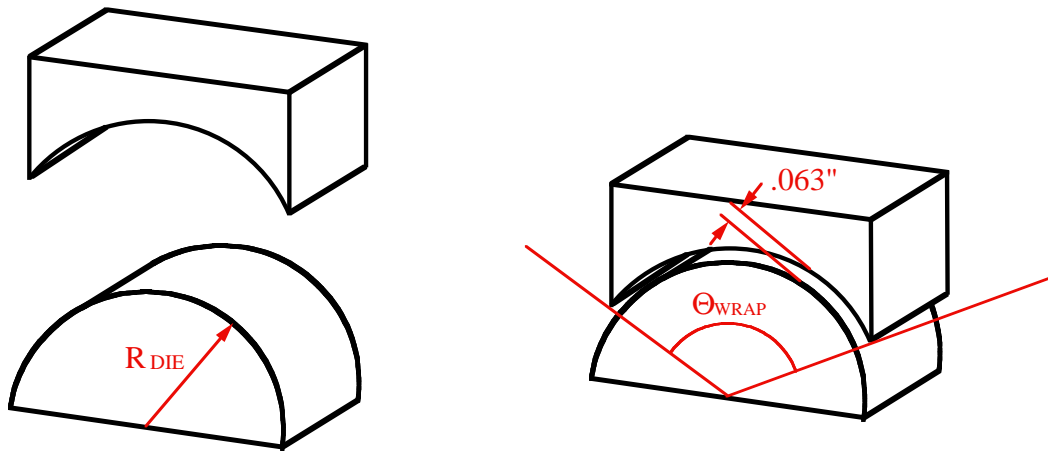


Figure 1: Schematic illustration of a matching die pair for imposing a single, constant curvature on a strip.

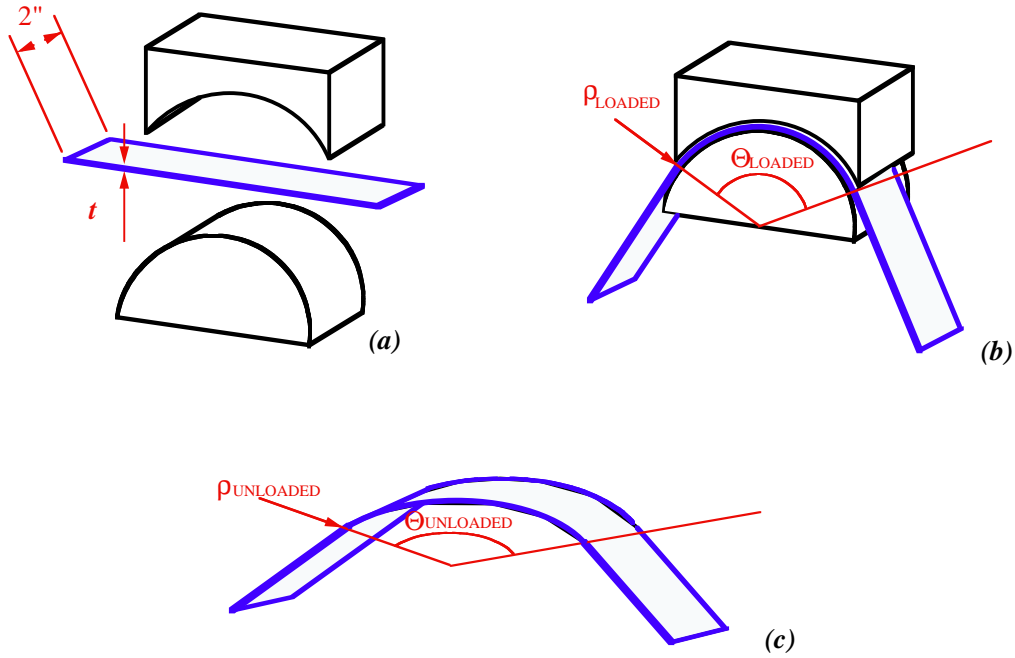


Figure 2: Schematic illustration of matching die sheet-forming process including (a) inserting the strip into the die; (b) closing the die onto the strip; and (c) the shape of the unloaded strip after the die has been opened and the strip removed from the die.

Strain gages have been applied to the surface of 6061 Aluminum alloy strips, cut to the approximate dimensions of  $2\text{ in}$  by  $12\text{ in.}$ , from sheet stock of thicknesses  $1/32\text{ in}$  and  $1/16\text{ in}$ , respectively. Moreover, the 6061 alloy strips are available in two different metallurgical conditions, owing to different heat-treatment histories. One heat-treated condition of the 6061 alloy is termed “T6”; this is a precipitation-hardened condition leading to elevated values of yield strength. The other heat-treated condition of the 6061, termed “T0”, is called “solution-annealed”; in this condition the strengthening precipitate particles have been dissolved into the matrix, followed by cooling, resulting in lower levels of yield strength.

The strips will be deformed by wrapping them around the surfaces of cylindrical male dies having radii of  $4\text{ cm}$  and  $8\text{ cm}$ , respectively. We will record the surface strains in the loaded and unloaded configurations on the  $4\text{ cm}$  die, and compare these measurements to predictions obtained using elastic-plastic beam-bending theory. We will also measure the resulting radii of curvature of various sheets after they have been removed from a closed die of radius  $8\text{ cm}$ , and compare these with predictions based on an idealized moment/curvature relation for each material/thickness combination tested.

## 2 Lab Tasks

In this laboratory we will perform the following tasks:

- review engineering models for elastic-plastic deformation, focusing on the elastic/perfectly-plastic (E/P-P) material model;
- review elastic-plastic beam-bending, including a discussion of the construction of the moment *vs.* curvature diagram for a beam of rectangular cross-section and elastic/perfectly-plastic material behavior;
- form the strain-gaged  $1/32$  in and  $1/16$  in thick 6061 Aluminum strips, of both heat treatments, on the circular cylindrical die of radius  $R_{\text{DIE}} = 300$  mm. Record and tabulate the surface strains in the loaded and unloaded configurations. Measure the radius of curvature of the formed strips in the unloaded configuration;
- discuss the effects of sheet thickness, Young's modulus, and yield strength on the magnitude of the elastic springback;
- perform a sheet metal forming experiment to observe the effects of sheet thickness and material properties on springback. For this experiment, we will consider a matching die with a single, constant radius of curvature,  $R_{\text{DIE}} = 8$  cm, and a wrapping angle,  $\Theta_{\text{WRAP}} = 90^\circ$  (See Fig. 1). We will use this die to form sheet metal strips 2 in wide and 12 in long, as schematically shown in Fig. 2. We will form five (5) different sheet materials: 6061-T6 Al in  $1/32$  in and  $1/16$  in thicknesses; solution-annealed 6061 Al in the same thicknesses; and a 1020 steel in  $1/16$  in [nominal] thickness, and measure the resulting radii of curvature of each strip in the unloaded configuration.
- compare the experimentally-measured radius of curvature for the unloaded strips with theoretical predictions obtained from a model moment/curvature relationship for each strip, based on an elastic/perfectly-plastic idealization of each material's behavior. The resulting model moment/curvature relations for the 6061-T6 Al strip and for 1020 steel in  $1/16$  in [nominal] thickness are shown in Fig. (6) and Fig. (7), respectively.

### 3 Lab Assignment: Specific Questions to Answer

1. Consider the 2 *in.* by 12 *in.* 6061-T6 Al strips in 1/32 *in.* and 1/16 *in.* thickness stock, which have been strain-gaged. Obtain a theoretical prediction for the strain at the outer surface of the strip when the strip is bent around the cylindrical die of radius 300 *mm.* How do the predictions compare with the strain levels measured by the gages?
2. Using the engineering theory of beam bending, calculate the elastic limit moment,  $M_e$ , of the 1/16 *in.* and 1/32 *in.*-thick strips of the 6061-T6 aluminum. Using an elastic/perfectly-plastic idealization of the behavior of the 6061-T6 alloy, plot the evolution of the bending moment,  $M$ , versus the strip curvature at its neutral axis,  $1/\rho \equiv \kappa$ , for both strips. The sheet will be in the elastic range for  $M \leq M_e$ , and in the elastic-plastic range for  $M > M_e$ . Plot the loading portion of the curve up to a loaded curvature  $\kappa_L \equiv (1/\rho_L) = 30 \text{ m}^{-1}$ .
3. Based on the moment/curvature diagrams obtained in (2), predict the (unloaded) radius of curvature,  $\rho_U = 1/\kappa_U$ , of the strips when they are unloaded from the 4 *cm.* radius die, and predict the unloaded surface strain. How do these predictions compare with the experimental measurements?
4. Predict the unloaded curvatures,  $\kappa_U$ , for all five materials when the sheets are formed in the 8 *cm.*-radius closed die. Discuss the effects of sheet thickness, yield strength, and elastic modulus on springback.
5. Is the overall accuracy of the springback calculation for the steel specimens of a level comparable to that of the aluminum ones? If not, what features of the steel are most likely responsible? Can you suggest ways to improve your predictions for springback in the steel specimens? Discuss. (But don't actually undertake any refined modeling derivations or calculations!)

## 4 Elastic-plastic beam-bending

See also, Crandall, Dahl, & Lardner, section 7.10 and/or Dowling, sections 13.2-13.3

### 4.1 Overview

The in-service use of most engineering structures involves loading levels sufficiently small so that only linear elastic deformation occurs. However, understanding structural behavior under larger loadings, *i.e.*, those sufficient to produce plastic deformation within the structure, is also important for assessing in-service structural behavior under accidental/unintended “overloads”, as well as for understanding manufacturing operations based on **deformation processing**.

In order to analyze this problem, we follow our solid mechanics fundamentals, by studying the geometry of deformation, the equilibrium of force, moments and stresses, and a constitutive model of elastic-plastic stress-strain behavior.

### 4.2 Geometry of straining

For pure bending of a rectangular cross-section of height  $h$  in the local  $y$ -direction, and width  $b$  in the local  $z$ -direction, with axis origin passing through the section centroid, the resulting strain distribution gives the axial strain varying linearly with  $y$ :

$$\epsilon_{xx}(y) = -\kappa y = -y/\rho. \quad (4.1)$$

This variation is plotted in Fig.(3) for two different curvature values.

### 4.3 Moment equilibrium

The bending moment equals the weighted area integral of the stress:

$$M = - \int_A y \sigma_{xx}(y) dA. \quad (4.2a)$$

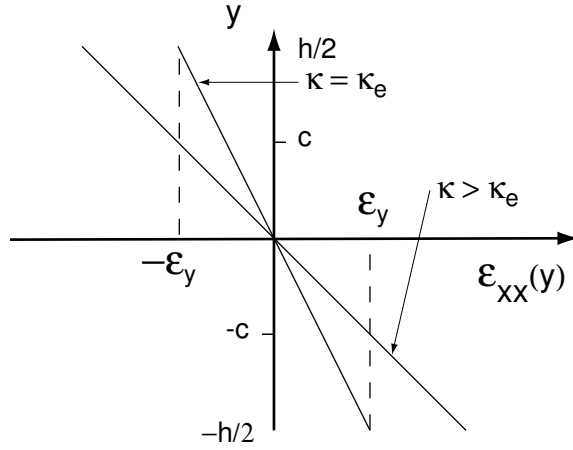


Figure 3: Linear through-thickness variation of axial strain  $\epsilon_{xx}(y)$  at two different values of imposed curvature,  $\kappa = \kappa_e$  and  $\kappa > \kappa_e$ . The curvature measure  $\kappa_e$  is introduced (see also, eq. (4.6), below), such that, if  $\kappa < \kappa_e$ , then  $|\epsilon_{xx}| < \epsilon_y = \sigma_y/E$  for all locations  $|y| \leq h/2$ .

Since  $dA = dy dz$ , and the stress varies only with  $y$ ,

$$M = -b \int_{-h/2}^{h/2} y \sigma_{xx}(y) dy. \quad (4.2b)$$

#### 4.4 Constitutive model

We have seen that linear elasticity connects uniaxial stress to strain according to

$$\sigma_{xx} = E \epsilon_{xx}, \quad (4.3)$$

providing stress is less than yield. Although we have yet not performed compression tests, it is generally found that the absolute value of the yield stress in compression (a negative number) is the same as in tension:  $\sigma_{y(c)} = -\sigma_{y(t)} = -\sigma_y$ . Here the subscripts “(t)” and “(c)” denote tension and compression, respectively.

For monotonically increasing strain magnitudes, another way to delimit the initial range of applicability of linear elastic stress-strain behavior is to note that it is limited to regions where  $|\epsilon_{xx}| \leq \epsilon_y$ , where the initial yield strain is  $\epsilon_y \equiv \sigma_y/E$ . This limitation on strain assures that  $|E\epsilon_{xx}| < \sigma_y$ .

The elastic-plastic tensile behavior past yielding shows various types of behavior, including strain hardening. However, a key feature of plasticity is that once plastic flow begins, the slope of the stress-strain curve,  $E_{\text{tangent}} \equiv d\sigma/d\epsilon$  quickly decreases to values far less than elastic modulus  $E$ :  $E_{\text{tangent}} \ll E$ . One widely-used mathematical model of this drastic reduction in slope of the stress-strain curve is the elastic/perfectly-plastic idealization that takes  $E_{\text{tangent}} = 0$ , resulting in increasing plastic strain at a fixed value of stress, namely  $\sigma = \pm\sigma_y$ , where the plus/minus refers to cases of tension/compression. A schematic of this idealized relation is shown in Fig.(4).

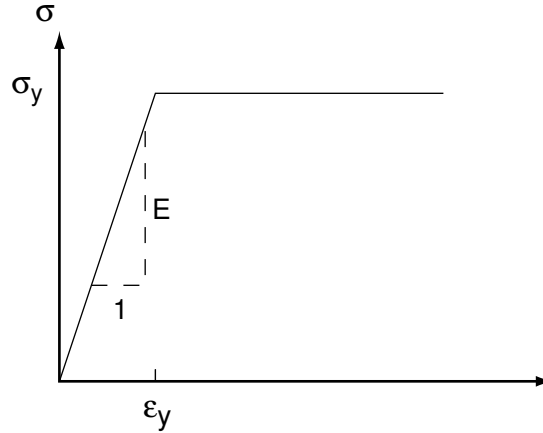


Figure 4: Tensile stress/strain curve of the elastic/perfectly-plastic material model under monotonically increasing imposed strain.

We can then summarize the stress versus strain response of the mathematical model of material behavior under monotonically-increasing magnitudes of strain magnitude,  $|\epsilon_{xx}|$ , by

$$\sigma_{xx} = \begin{cases} E\epsilon_{xx} & \text{if } |\epsilon_{xx}| \leq \epsilon_y \equiv \sigma_y/E \\ \sigma_y & \text{if } \epsilon_{xx} > \epsilon_y \\ -\sigma_y & \text{if } \epsilon_{xx} < -\epsilon_y. \end{cases} \quad (4.4)$$

Returning now to the beam-bending problem, in evaluating the  $y$ -dependence of  $\sigma_{xx}(y)$  within eq.(4.2b), we substitute the  $y$ -dependence of strain,  $\epsilon_{xx}(y) = -y\kappa = -y/\rho$  into the expression (4.4) for elastic/perfectly-plastic stress/strain behavior. Of course, the magnitude of strain, which delineates which of the expressions to use for the stress value, depends on both position in the section, through  $y$ , and on the magnitude of imposed deformation, the curvature  $\kappa$ . Accordingly, we will find it useful to develop relations between  $M$  and  $\kappa$ .

## 4.5 Moment-curvature relation: loading

We start with linear elastic response throughout the cross-section. This requires  $\kappa$  to be sufficiently small (this is made quantitative below), and results in

$$M = -b \int_{-h/2}^{h/2} E(-\kappa y) y dy = E \frac{bh^3}{12} \kappa = EI\kappa. \quad (4.5)$$

For fixed  $\kappa$ , the maximum magnitude of strain occurs at the top and bottom fibers,  $y = \pm h/2$ , where the corresponding strains are  $\epsilon_{xx} = \mp \kappa h/2$ . In order for these largest strain magnitudes to be less than the yield strain  $\epsilon_y$ , it is necessary that  $\kappa$  satisfy

$$\kappa \leq \kappa_e,$$

where

$$\kappa_e \equiv \frac{\epsilon_y}{h/2} = \frac{2\sigma_y}{Eh} \quad (4.6)$$

is the limiting value of curvature for purely linear elastic response.

The value of the moment at this elastic limit point is

$$M_e = EI\kappa_e = EI \frac{2\sigma_y}{Eh} = \frac{2\sigma_y I}{h} = \frac{bh^2}{6} \sigma_y. \quad (4.7)$$

Now suppose that  $\kappa$  increases beyond  $\kappa_e$ ; the strain still varies linearly through the section, but  $|\epsilon_{xx}(y)| \geq \epsilon_y$  over a certain region  $c \leq |y| \leq h/2$ , where (see also Fig. (3))  $c > 0$  is the magnitude of the  $y$ -coordinate of the transition between elastic behavior (for  $|y| \leq c$ ) and plastic behavior (for  $h/2 \geq |y| \geq c$ ). We can solve for  $c$  in terms of  $\kappa$  by recognizing that  $|\epsilon_{xx}(y = \pm c)| = \epsilon_y$ : for the tension side, at  $y = -c$ ,

$$\kappa c = \epsilon_y \quad (4.8)$$

so that

$$c(\kappa) = \frac{\epsilon_y}{\kappa} \quad (\text{for } \kappa \geq \kappa_e). \quad (4.9)$$

For any given curvature  $\kappa \geq \kappa_e$ ,  $c(\kappa)$  represents the half-thickness of the remaining “elastic core” of the beam. Thus, in terms of  $c(\kappa)$ , the  $y$ -dependence of stress in the elastic-plastic regime is:

$$\sigma_{xx}(y) = \begin{cases} \sigma_y & \text{in } -h/2 \leq y \leq -c \\ -E\kappa y & \text{in } -c \leq y \leq c \\ -\sigma_y & \text{in } c \leq y \leq h/2. \end{cases} \quad (4.10)$$

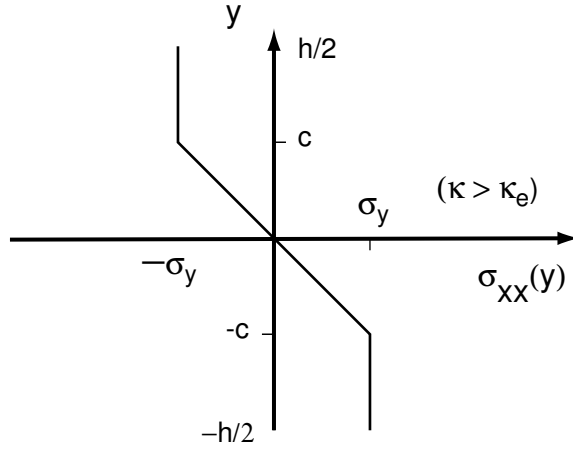


Figure 5: Schematic through-thickness stress variation in a rectangular beam of elastic/perfectly-plastic material, loaded into the elastic-plastic regime, Equation (4.10).

Inserting (4.10) into (4.2), the integral for moment becomes

$$\begin{aligned}
 M &= -b \left[ \int_{-h/2}^{-c} \sigma_y y \, dy + \int_{-c}^c -E\kappa y^2 \, dy + \int_c^{h/2} -\sigma_y y \, dy \right] \\
 &= \frac{Eb\kappa c^3}{3} + \sigma_y b \left( \left( \frac{h}{2} \right)^2 - c^2 \right). \quad (4.11)
 \end{aligned}$$

Substituting in the value  $E\kappa c = \sigma_y$  for one power of “ $c$ ” in the term containing “ $c^3$ ,” and then collecting terms, provides

$$M = b\sigma_y \left( \frac{h^2}{4} - \frac{c^2}{3} \right) \quad (\text{for } \kappa \geq \kappa_e). \quad (4.12)$$

In the fully-plastic limit, as  $\kappa$  grows large and  $c \rightarrow 0$ , the value of  $M$  in eq. (4.12) converges to an asymptotic, fully-plastic limiting value given by

$$M \rightarrow M_p = \frac{bh^2}{4} \sigma_y = \frac{3}{2} M_e. \quad (4.13)$$

Also, at the nearly-elastic limit of  $\kappa \rightarrow \kappa_e^+$  and  $c \rightarrow (h/2)^-$ , eq. (4.12) recovers the value  $M \rightarrow M_e = 2M_p/3$  as before.

Summarizing, the moment/curvature relation for monotonically increasing applied curvature can be expressed using two branches as

$$M(\kappa) = \begin{cases} E b h^3 \kappa / 12 & \text{if } \kappa \leq \kappa_e \equiv 2\sigma_y / E h \text{ (elastic)} \\ (b h^2 \sigma_y / 4) (1 - (\kappa_e / \kappa)^2 / 3) & \text{if } \kappa \geq \kappa_e \text{ (elastic-plastic)}. \end{cases} \quad (4.14)$$

Figures (6) and (7) graph  $M$ - $\kappa$  relations calculated from eq. (4.14) for specific cases of material properties ( $E$ ;  $\sigma_y$ ) and geometry ( $h$ ;  $b$ ).

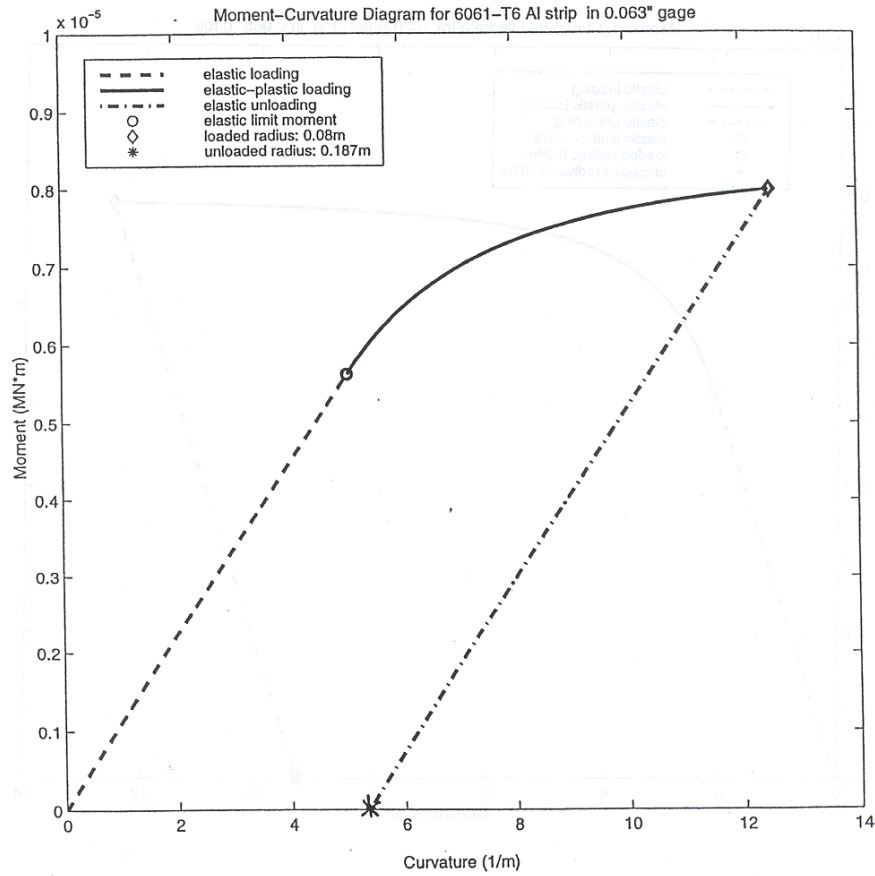


Figure 6: Model elastic/perfectly-plastic moment ( $M$ ) vs. curvature ( $\kappa$ ) relationship for Aluminum 6061-T6 sheet  $h = 1/16$  in. thick and  $b = 2.0$  in. wide, calculated using eq. (4.14). ( $E = 70$  GPa;  $\sigma_y = 275$  MPa).

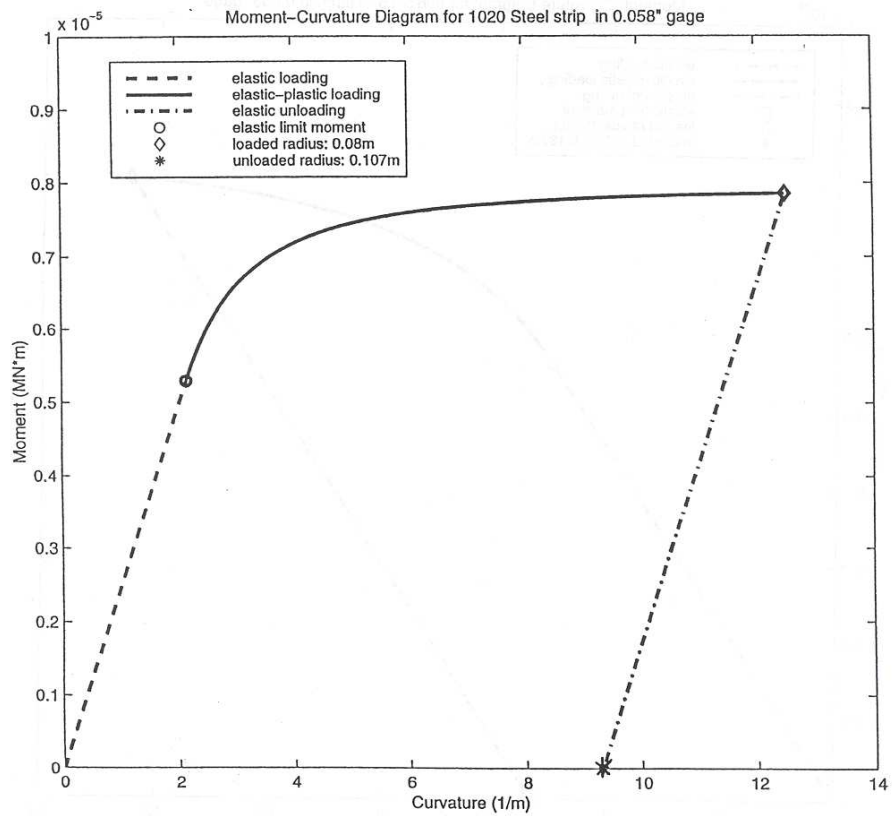


Figure 7: Model elastic/perfectly-plastic moment ( $M$ ) vs. curvature ( $\kappa$ ) relationship for 1020 steel sheet  $h = 0.058 \text{ in.}$  thick ( $1/16 \text{ in}$  nominal) and  $b = 2.0 \text{ in.}$  wide, calculated using eq. (4.14). ( $E = 208 \text{ GPa}$ ;  $\sigma_y = 300 \text{ MPa}$ ).

## 4.6 Unloading after plastic bending and residual stress pattern

Under large-scale plastic bending, the moment can build up to values as large as 1.5 times the elastic limit value,  $M_e$ . What happens to the stress and the strain when the moment is decreased to zero (unloading) after first loading to some point  $(M_{(\text{loaded})}, \kappa_{(\text{loaded})})$  in the elastic-plastic regime? At least initially, the material deforms elastically on unloading after plastic deformation; *i.e.*,  $\Delta\sigma_{xx} = E \Delta\epsilon_{xx}$ , where the notation “ $\Delta$ ” denotes the change, following unloading. That is,

$$\Delta(\dots) \equiv (\dots)_{(\text{unloaded})} - (\dots)_{(\text{loaded})}. \quad (4.15)$$

For example, the change in moment is  $\Delta M = 0 - M_{(\text{loaded})} = -M_{(\text{loaded})}$ , using the obvious value  $M_{(\text{unloaded})} \equiv 0$ . Moreover, letting the corresponding change in the stress field be  $\Delta\sigma_{xx}(y)$ , moment equilibrium (change) requires

$$\Delta M = - \int_A y \Delta\sigma_{xx}(y) dA. \quad (4.16)$$

Returning to the question, we assume that, during unloading, there will be a change in curvature,  $\Delta\kappa$ , that generates a change in the strain field given by

$$\Delta\epsilon_{xx}(y) = -y\Delta\kappa. \quad (4.17)$$

If elastic response holds for the entire unloading step (all the way to  $M_{(\text{unloaded})} = 0$ ), we can substitute the elastic unloading relation  $\Delta\sigma_{xx}(y) = E\Delta\epsilon_{xx}(y) = -Ey\Delta\kappa$  to obtain

$$\Delta M = EI \Delta\kappa, \quad (4.18a)$$

or

$$\Delta\kappa = \frac{\Delta M}{EI} = -\frac{M_{(\text{loaded})}}{EI}. \quad (4.18b)$$

Thus, the unloaded curvature must be

$$\kappa_{(\text{unloaded})} = \kappa_{(\text{loaded})} + \Delta\kappa = \kappa_{(\text{loaded})} - \frac{M_{(\text{loaded})}}{EI}. \quad (4.19)$$

If we desire a particular value of curvature to remain after unloading ( $\kappa_{(\text{unloaded})}$ ), then we must choose the value of (maximum) loaded curvature to impose during forming, since the loaded bending moment,  $M_{(\text{loaded})}$ , itself depends on the loaded curvature, material properties, and geometry through eq. (4.14).

Once we have determined  $\Delta\kappa$ , and thus  $\kappa_{(\text{unloaded})}$ , the unloaded strain field follows trivially as

$$\epsilon_{xx(\text{unloaded})}(y) = -y\kappa_{(\text{unloaded})}. \quad (4.20)$$

But now comes a “moment of truth”, for, to this point, we have merely assumed that elastic behavior described material response throughout the unloading process. In order to verify our assumption, we must compute the final, unloaded stress field throughout the section, making sure that no point in the body has a stress violating the yielding inequality  $|\sigma_{xx(\text{unloaded})}| \leq \sigma_y$ . If the inequality is satisfied, our assumption was right and we have the correct answer, but if not, we would need to revise our assumptions and work some more. Mercifully, it turns out that the assumption is correct. Let’s see how.

From our provisional elastic unloading assumptions,

$$\begin{aligned}
\sigma_{xx(\text{unloaded})}(y) &= \sigma_{xx(\text{loaded})}(y) + \Delta\sigma_{xx}(y) \\
&= \sigma_{xx(\text{loaded})}(y) - Ey\Delta\kappa \\
&= \sigma_{xx(\text{loaded})}(y) + Ey(M_{(\text{loaded})}/EI) \\
&= \sigma_{xx(\text{loaded})}(y) + yM_{(\text{loaded})}/I.
\end{aligned} \tag{4.21}$$

Eq. (4.21) can be evaluated for any value of  $\kappa_{\text{loaded}}$  and corresponding “loaded” moment  $M_{(\text{loaded})}$  and “loaded” stress distribution  $\sigma_{xx(\text{loaded})}(y)$ . Here we show that, even at the limiting state of  $\kappa_{(\text{loaded})} \rightarrow \infty$  and  $M_{(\text{loaded})} \rightarrow M_p = \sigma_y bh^2/4$ , the resulting unloaded stress state obtained from eq. (4.21) is everywhere less than or equal to  $\sigma_y$  in magnitude; that is, the resulting unloaded stress at no place exceeds the material’s yield condition. The limit-value of  $M_p$  occurs when  $c \rightarrow 0$ , in which case the fully-plastic loaded stress state is simply

$$\sigma_{xx(\text{loaded})}(y) \rightarrow \sigma_{xx(\text{fully-plastic})}(y) \equiv \begin{cases} \sigma_y & \text{if } -h/2 \leq y < 0 \\ -\sigma_y & \text{if } 0 < y \leq h/2. \end{cases} \tag{4.22}$$

Since  $I = bh^3/12$ ,  $yM_p/I = 3\sigma_y y/h$  and, on using these values and eq. (4.22), we can substitute into eq. (4.21) to obtain

$$\sigma_{xx(\text{unloaded})}(y) = \begin{cases} \sigma_y + 3\sigma_y(y/h) & \text{if } -h/2 \leq y < 0 \\ -\sigma_y + 3\sigma_y(y/h) & \text{if } 0 < y \leq h/2. \end{cases} \tag{4.23}$$

This unloaded, or “residual,” stress field has a surprising shape, shown in Fig. (8). At the top surface,  $y = h/2$ , its value is  $\sigma_y/2$ , and it varies linearly with  $y$  down to  $-\sigma_y$  at  $y = 0^+$ . Similarly, its value on the bottom surface,  $y = -h/2$ , is  $-\sigma_y/2$ , varying linearly with  $y$  up to a value of  $\sigma_y$  at  $y = 0^-$ . Nowhere does the residual (unloaded) stress state exceed  $\sigma_y$  in magnitude! Our assumption of elastic unloading proved correct, so our answer is also correct.

It is important to realize that in this example, there is a *non-zero residual stress distribution* in the beam, even though there is *zero external force and moment*. That is,

$$N_{(\text{unloaded})} = 0 = \int_A \sigma_{xx(\text{unloaded})} dA; \tag{4.24a}$$

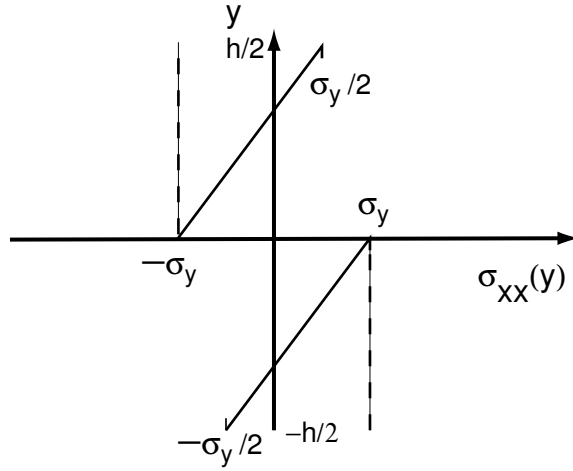


Figure 8: Unloaded (residual) stress variation through-thickness after unloading from a fully-plastic state ( $M \rightarrow M_p$ ;  $\kappa \rightarrow \infty$ ; etc.) in the elastic/perfectly-plastic model, as calculated from Eq. (4.23).

$$M_{(\text{unloaded})} = 0 = - \int_A y \sigma_{xx(\text{unloaded})} dA. \quad (4.24b)$$

This is completely different from the zero-valued residual stress which occurs when a uniformly-strained tensile bar is unloaded after plastic deformation: the key difference is the spatially inhomogeneous plastic deformation associated with the original bending.

## 4.7 Summary

We have systematically outlined and derived the steps in the stress analysis of elastic-plastic beam bending and unloading. A final (color) graphic, Fig. 9, summarizes essential relations among all the field variables. Note, however, that the this figure assumes that the  $y$ -component of stress varies with coordinate  $x$  (a rotated beam).

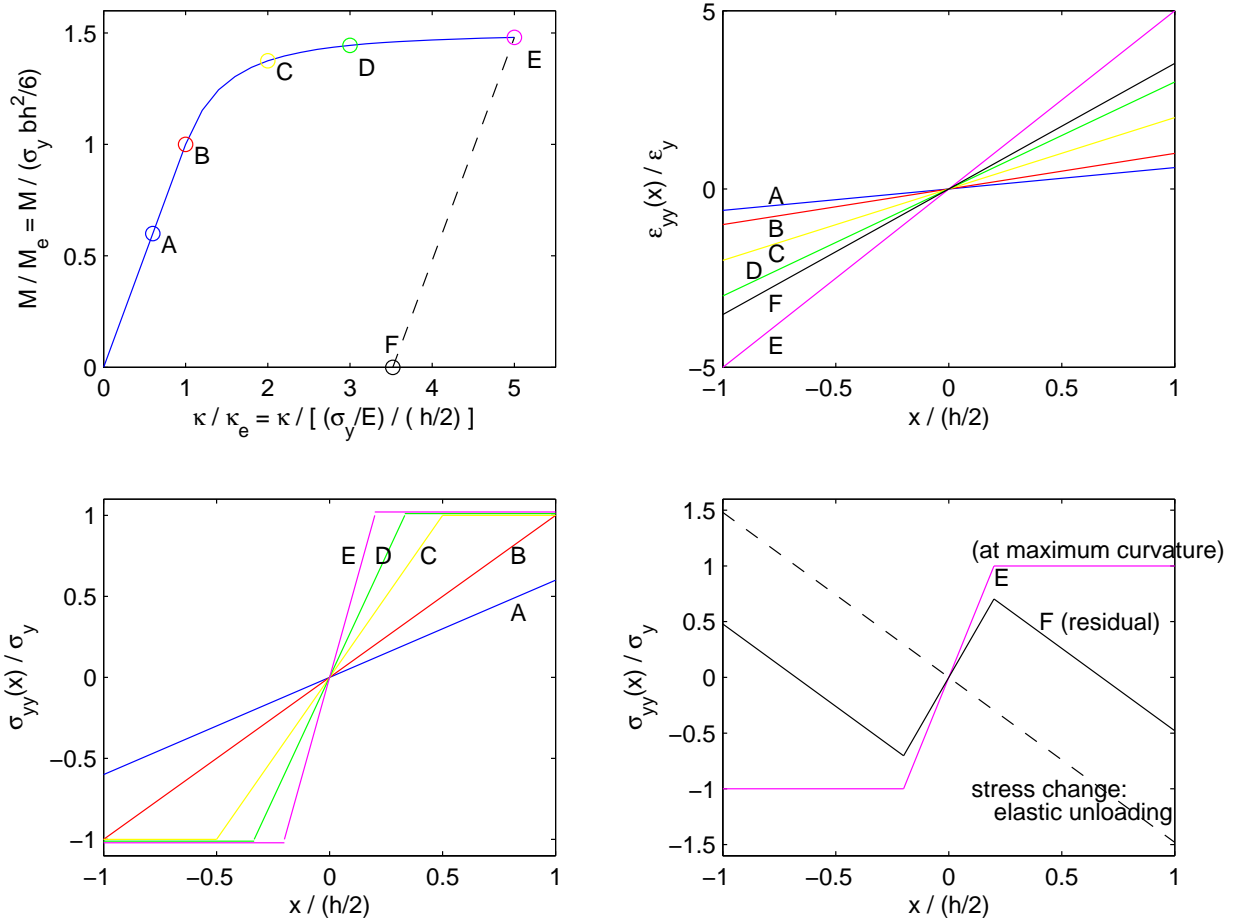


Figure 9: Four-panel color graphic summary of elastic-plastic bending and unloading. (Note: in this figure, the beam being bent is aligned along the  $y$ -axis, instead of the  $x$ -axis, which was used elsewhere in the document.)